Received 21 January 2015; revised 5 February 2015, 25 February 2015, 2 April 2015, and 19 April 2015; accepted 20 April 2015. Date of publication 4 May 2015; date of current version 19 June 2015. The review of this paper was arranged by Editor A. G. Unil Perera.

Digital Object Identifier 10.1109/JEDS.2015.2428993

Uniform Luminescence at Breakdown in 4H-SiC 4°-Off (0001) p–n Diodes Terminated With an Asymmetrically Spaced Floating-Field Ring

KAZUHIRO MOCHIZUKI[1,2] (Senior Member, IEEE), NORIFUMI KAMESHIRO[3], HIROYUKI MATSUSHIMA[2], HIROYUKI OKINO[2,4], AND RENICHI YAMADA[2] (Senior Member, IEEE)

1 Advanced Power Electronics Research Center, National Institute of Advanced Industrial Science and Technology, Tsukuba 305-8568, Japan
2 Center for Technology Innovation–Electronics, Hitachi, Ltd., Tokyo 185-8601, Japan
3 Center for Exploratory Research, Hitachi, Ltd., Tokyo 185-8601, Japan
4 Hitachi Power Semiconductor Device, Ltd., Hitachi 319-1221, Japan

CORRESPONDING AUTHOR: K. MOCHIZUKI (e-mail: k-mochiduki@aist.go.jp)

ABSTRACT Conventional floating-field rings, which are used to reduce the peak electric field at the periphery of power devices, cause nonuniform avalanche multiplication when applied to planar junctions formed on 4H-SiC substrates misoriented from (0001) toward [11$\bar{2}$0]. Accordingly, a novel asymmetrically spaced floating-field ring (AS-FFR) was applied to 4H-SiC 4°-off (0001) p–n diodes and found to be effective against such nonuniform avalanche multiplication; that is, luminescence at breakdown was nearly uniform when the spacing between the edge of the anode and the inner edge of the AS-FFR was 2.0 μm in the [$\bar{1}\,\bar{1}$20] direction and 1.5 μm in the [11$\bar{2}$0] direction. This result should contribute to exploring the possibility of 4H-SiC power devices with higher avalanche ruggedness.

INDEX TERMS Aluminum, ion implantation, power semiconductor devices, silicon compounds.

I. INTRODUCTION

4H-silicon carbide (SiC) is an attractive material for high-voltage and high-frequency power devices [1]–[3]. Robust 4H-SiC devices can only be fabricated by using a properly designed termination structure that reduces the peak electric field at the periphery of a device [4]. Among the possible termination structures, floating-field rings (FFRs) [5] are often used because of the simplicity of their fabrication process; however, FFRs were reported to cause non-uniform avalanche multiplication when applied to planar junctions formed on misoriented (0001) substrates [6], [7].

Misorienting a 4H-SiC (0001) substrate is indispensable for step-flow epitaxial growth of 4H-SiC [8]. Aluminum acceptors vertically implanted into a misoriented substrate should thus have asymmetric profiles due to the negligible diffusion of aluminum [9]–[13]. Such asymmetric acceptor profiles are considered to cause the non-uniform avalanche multiplication in 4H-SiC 4°-off (0001) p-n diodes terminated with a conventional concentric FFR [7].

In the case of merged pn-Schottky diodes terminated with junction termination extension (JTE), continuous avalanche test was reported to form a burn spot when luminescence was observed only at one side of the JTE [14]. Avalanche multiplication in termination region should thus be as uniform as possible, even in the case of FFRs. In this study, a novel asymmetrically spaced FFR (AS-FFR), which was designed based on the recently proposed numerical-analysis methodologies [15], [16], was applied to 4H-SiC 4°-off (0001) p-n diodes. The resultant nearly uniform luminescence at breakdown should contribute to exploring the possibility of higher avalanche ruggedness.

II. SIMULATION

A schematic device-simulated structure of a p-n diode terminated with a 5-μm-wide FFR is shown in Fig. 1(a). The structure is similar to that proposed by Cheng et al. for calculating the "*BV-spacing curve*" for the optimal

FFR [15], except for the etched surface. Etching the 4H-SiC (0001) surface to expose the experimentally used 4° misoriented (0001) surface is necessary [16] since the surface orientation is on-axis (0001) in such commercial device simulators as Sentaurus Device [17] and ATLAS [18]. Structures A and B, respectively, represent an FFR in the $[\bar{1}\,\bar{1}20]$ direction and an FFR in the $[11\bar{2}0]$ direction (i.e., the off direction). In both structures, only the outer part of the anode and the inner part of the FFR are included [15]. The anode and a 5-μm-wide FFR were simultaneously formed by Monte Carlo simulation of four-fold aluminum implantation (at room temperature) normal to the wafer surface under the following conditions: 145 keV/1.0×10^{14} cm^{-2}, 95 keV/3.5×10^{13} cm^{-2}, 60 keV/3.0×10^{13} cm^{-2}, and 35 keV/1.5×10^{13} cm^{-2} [16].

The breakdown behavior of a junction, which is protected by an FFR with a spacing *d'*, was simulated at room temperature by assuming vectorial driving forces [17] (with anisotropic impact ionization coefficients α reported by Hatakeyama *et al.* [19]) and a sheet fixed-charge density at the SiO_2/4H-SiC interface of 2×10^{12} cm^{-2} [16]. The simulated drift layer had a thickness of 30 μm and a donor density of 2.9×10^{15} cm^{-3}.

Fig. 1(b) and (c) shows the simulated "*BV-spacing curve*" [15], where breakdown voltage of negatively-biased anode is shown as a function of *d'*. The effective reverse bias of FFR represents the electrostatic potential of FFR when the anode undergoes avalanche breakdown. Note here that Fig. 1(b) and (c) shows the breakdown voltage of structures A and B, not the breakdown voltage of the real device structure having the outer half of FFR. Therefore, the value of vertical axis cannot be directly compared at a fixed value of horizontal axis.

As explained by Chen *et al.* [15], the breakdown voltage of anode (*BV*) decreases with the increase of *d'* because of a less protection from the FFR. And when *d'* becomes very large (> 3.5 μm) [Fig. 1(b) and (c)], *BV* will decrease to its cylindrical junction value. Under the optimized breakdown condition, the effective reverse bias of FFR thus becomes this cylindrical junction value. The effective reverse bias of FFR becomes 200 V at a *d'* of 2.0 μm in structure A [Fig. 1(b)] and 210 V at a *d'* of 1.6 μm in structure B [Fig. 1(c)]. These values of *d'* correspond to the optimal spacing. And when these values of *d'* are used, the optimized breakdown voltage of anode becomes 380 V in structure A and 390 V in structure B.

Due to the immaturity of two-dimensional Monte Carlo simulation, i.e., insufficient lateral straggling of aluminum, *BV* becomes less than half the experimental value, as shown as the simulated and measured *BV* at *d'* = 2.0 μm in Fig. 1(b). However, the difference in the simulated *BV* at *d'* = 2.0 and 4.0 μm (i.e., 180 V) and the difference in the measured *BV* at *d'* = 2.0 μm and infinity (i.e., 178 V) agree very well. Therefore, the optimal *d'* in the $[11\bar{2}0]$ direction is expected to be determined from Fig. 1(c), i.e., 1.6 μm.

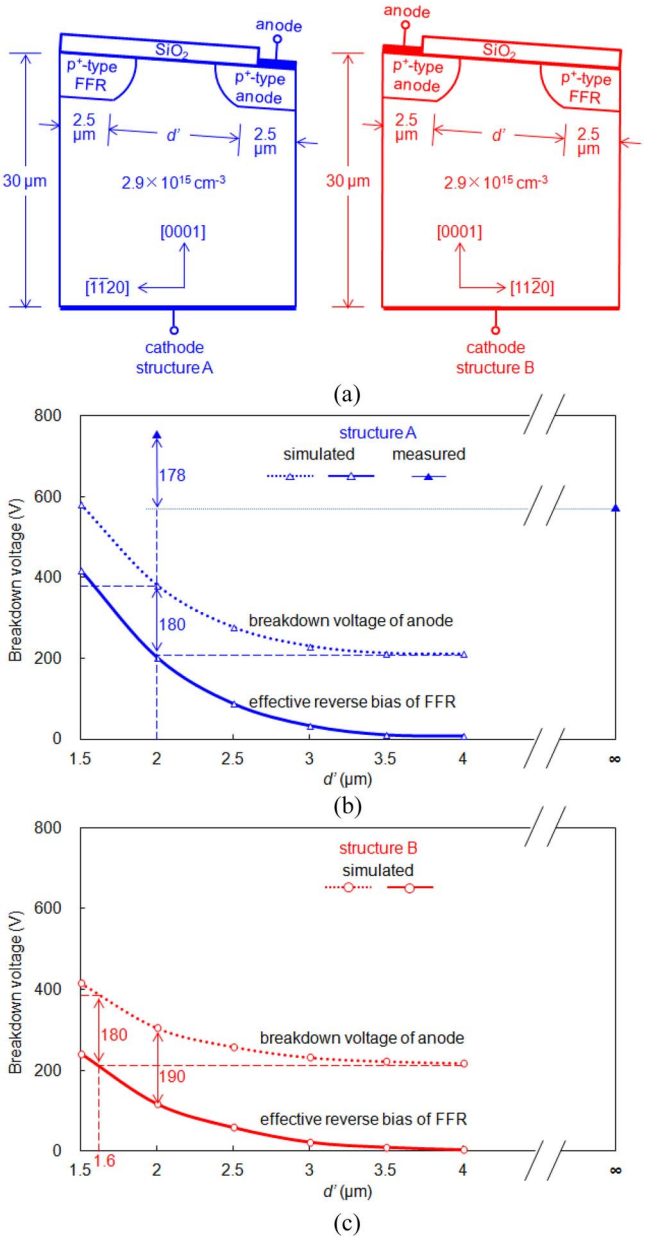

FIGURE 1. (a) Modeling structure used in simulation. (b) and (c) Simulated and measured breakdown voltage at RT as a function of spacing *d'*. The measured breakdown voltage at infinity shown in Fig. 1(b) represents the breakdown voltage of a p–n diode without FFR.

The difference between the above-described simulation result and a well-known result that when compared with the same *d'*, the *BV* of structure B is higher than the *BV* of structure A [7] can be understood as follows: When *d'* in structure B is decreased from 2.0 to 1.6 μm, the difference between the breakdown voltage of negatively-biased anode and the effective reverse-bias of FFR (Δ) decreases from 190 to 180 V [Fig. 1(c)]. Since the latter value of Δ coincides with Δ of *d'* = 2.0 μm in structure A [Fig. 1(b)], the resultant AS-FFR-terminated p-n diode has the same *BV* in structures A and B but consumes less termination area in structure B (Fig. 2).

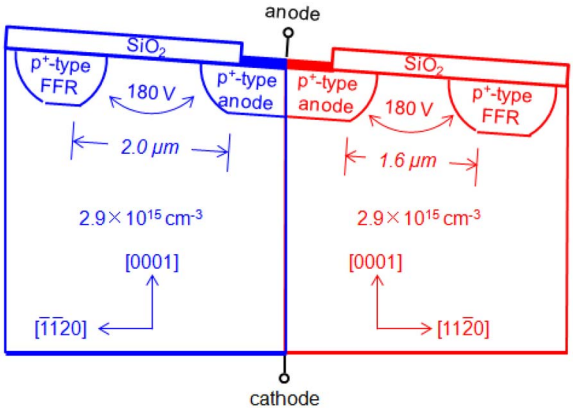

FIGURE 2. Schematic of AS-FFR-terminated p–n diode that consist of structures A and B [Fig. 1(a)] with the outer halves of each FFR.

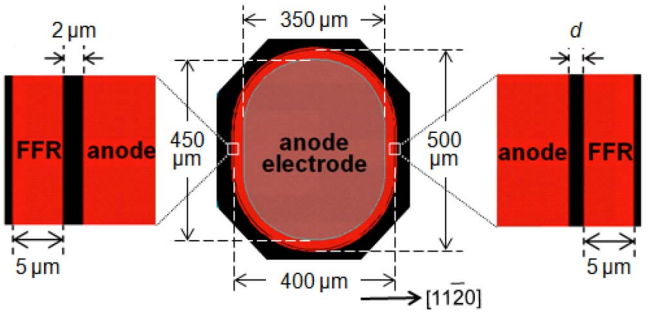

FIGURE 3. Plan view of a diode with spacing between the edge of the anode area and the inner edge of the floating-field ring of 2.0 μm in the $[\bar{1}\,\bar{1}20]$ direction and d (1.5, 1.6, 1.7, 2.0 μm) in the $[11\bar{2}0]$ direction. The major axes of p-type anode and anode electrode are, respectively, 500 and 450 μm long.

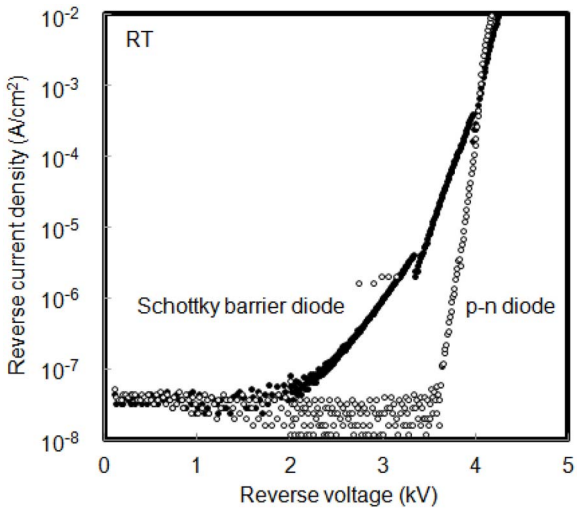

FIGURE 4. Example of reverse current density/voltage characteristics of Schottky barrier and p–n diodes, whose anode electrodes are non-Ohmic, terminated with conventional junction termination extension.

III. EXPERIMENTS

A schematic plan view of the fabricated AS-FFR-terminated 4H-SiC p-n diodes is shown in Fig. 3. Forty-eight diodes were fabricated on a 3-in 4H-SiC epitaxial wafer (with a 30-μm-thick drift layer) and doped with nitrogen donors at 2.9×10^{15} cm^{-3}. This epitaxial-layer specification corresponds to a drift layer of 3.3 kV-class power devices terminated with several FFRs [20]. In this study, a single FFR was chosen for simplicity, so the breakdown voltage becomes low (Section II); however, the luminescence at breakdown can be discussed because it is mainly affected by the peak electric field, not by the breakdown voltage itself. In the optimal structure, the peak electric field of an FFR-terminated p-n diode should be the same as that of a multiple FFR-terminated p-n diode [15].

The 4H-SiC substrate, the surface of which was misoriented by 4°±0.5° from (0001) toward the $[11\bar{2}0]$ direction, had a thickness of 350±25.4 μm and a resistivity of 0.015-0.025 Ωcm. An ellipsoidal anode was used to exclude possible avalanche multiplication around corners of the anode [6]. Its major axis was 500 μm long and parallel to the <1100> direction, while its minor axis was 400 μm long.

The anode and a 5-μm-wide AS-FFR were simultaneously formed by four-fold aluminum implantation at room temperature under the conditions described in the previous section. The resultant aluminum concentration was about 1×10^{19} cm^{-3} [7].

Spacing between the edge of the anode area and the inner edge of the AS-FFR in the $[\bar{1}\,\bar{1}20]$ direction was fixed at 2.0 μm (Section II). In the $[11\bar{2}0]$ direction, on the other hand, spacing (denoted by d in Fig. 3) between the edge of the anode area and the inner edge of the AS-FFR was varied from 1.5 to 2.0 μm.

After the implants were activated by annealing at 1700°C, the surface was passivated with dry oxidation. As front-side and backside electrodes, titanium and nickel contacts were formed, respectively. Since this study also aims at applying AS-FFR to junction-barrier Schottky diodes [21], the anode contact was non-Ohmic. However, even with such non-Ohmic anode electrode, BV can be precisely determined [22], as shown as an example in Fig. 4; BV of Schottky barrier and p-n diodes, whose anode electrodes were non-Ohmic, coincides when reverse current density exceeds 10^{-3} A/cm^2.

The visible-light emissions were observed, and the reverse current/voltage characteristics of the AS-FFR terminated diodes were measured at room temperature.

IV. RESULTS AND DISCUSSION

In agreement with a previously reported result [7], all 12 of the fabricated diodes with d of 2.0 μm emitted light at avalanche breakdown (BV = 748±1 V at reverse current I_R of 2 mA) on the $[\bar{1}\,\bar{1}20]$ side of the anode [Fig. 5(a) and dashed line in Fig. 6]. When reverse voltage is larger than 720 V in Fig. 6, reverse current density exceeds 10^{-1} A/cm^2, which is well beyond 10^{-3} A/cm^2 (Fig. 4). The luminescence shown in Fig. 5 is thus considered to correspond to avalanche multiplication. According to Ono et al., luminescence at

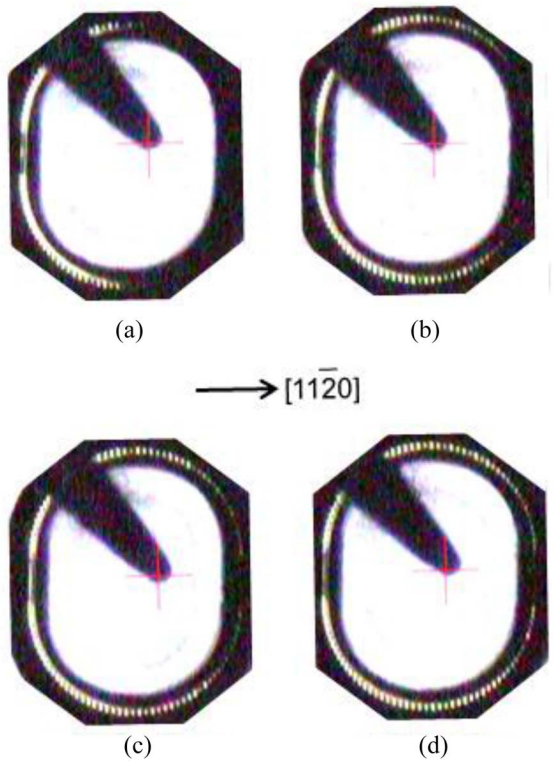

FIGURE 5. Photographically recorded light emissions from a floating-field-ring-terminated 4H-SiC p–n diodes operated at reverse current of 2 mA. (a) $d = 2.0$ μm. (b) $d = 1.7$ μm. (c) $d = 1.6$ μm. (a) $d = 1.5$ μm.

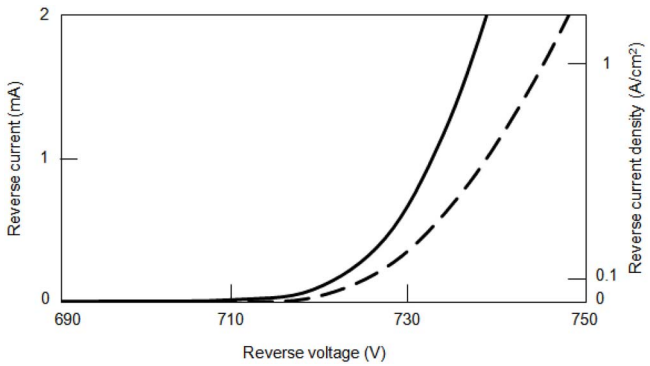

FIGURE 6. Examples of reverse current/voltage characteristics of fabricated p–n diodes terminated with a conventional FFR (dashed line) and an AS-FFR (solid line).

breakdown of 4H-SiC p-n diodes is attributable to band-to-band transition, interband transition, and Bremsstrahlung (braking radiation) by hot carriers in a Coulomb field of charged impurities [23].

It has to be repeated here that the simulated *BV* is less than half the measured *BV*. This is also the case with the *BV* simulated by assuming scalar driving forces [17] (with isotropic α reported by Konstantinov *et al.* [24]) [7]. These results indicate that the asymmetric nature of impact ionization [19] has little influence on the measured *BV* and that the simulated asymmetric aluminum concentration contours are not accurate enough to reproduce the measured *BV*.

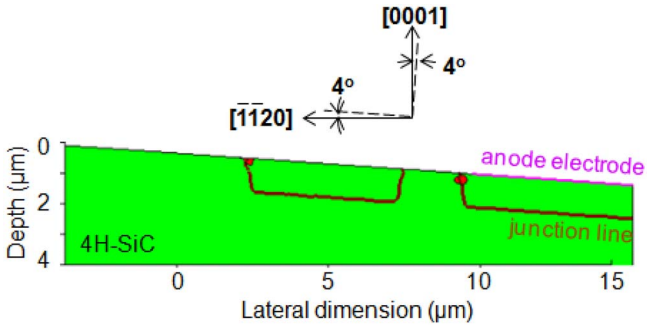

FIGURE 7. Simulated locations (red regions) where impact ionization rate exceeds 1×10^{19} cm^{-3}s^{-1} with an assumption of a sheet fixed-charge density at the SiO_2/4H-SiC interface of 2×10^{12} cm^{-2}, together with junction lines (brown lines), of p–n diode terminated with concentric FFR ($d = 2.0$ μm).

On the basis of the accuracy of one-dimensional Monte Carlo simulation [7], the real lateral straggling of aluminum is considered to be larger than the simulated one [16]. The accuracy of two-dimensional Monte-Carlo simulation thus needs to be improved. However, as stated in Section II, quantitative discussion on d is considered to be valid.

Fig. 7 shows the peak simulated impact ionization rate (R) at breakdown in the [$\bar{1}\,\bar{1}$20] direction of p-n diodes with d of 2.0 μm. The regions where R exceeds 1×10^{19} cm^{-3}s^{-1} have about the same cross section around the edge of the anode and around the outer edge of the FFR. Therefore, a half of I_R, i.e., 1 mA, can be considered to flow from the outer edge of the FFR toward the outer edge of the anode. This corresponds to a fairly large power density (about 200 kW/cm^2) on the [$\bar{1}\,\bar{1}$20] side of the device.

When d was reduced, luminescence at breakdown extended toward the other side (i.e., the [11$\bar{2}$0] direction) of the anode [Fig. 5(b)–(d) and solid line in Fig. 6]. Of all 36 of the diodes with $d < 2.0$ μm, *BV* was 738±3 V at $I_R = 2$ mA.

These results, together with the reported slightly temperature-dependent *BV* of 4H-SiC diodes [14], indicate that the part of the AS-FFR in the [11$\bar{2}$0] direction came to function as a FFR; thus, the increase in the temperature of the luminescent region in the [$\bar{1}\,\bar{1}$20] direction is less than that in the case of the conventional FFR. The slightly lower breakdown voltage of the fabricated diodes with reduced d thus indicates more rugged operation through avalanching in larger area with less temperature increase.

When d was 1.5 μm and I_R was increased to 10 mA, nearly uniform light emission was observed around the whole outer edge of the AS-FFR (denoted by A and C in Fig. 8) as well as from the edge of the anode in the [$\bar{1}\,\bar{1}$20] direction (denoted by B in Fig. 8). The results shown in Figs. 5 and 6 indicate that region C would function more effectively as a FFR if d were decreased to less than 1.5 μm. This result also supports the need for improvement of the accuracy of two-dimensional Monte Carlo simulation described in Section II.

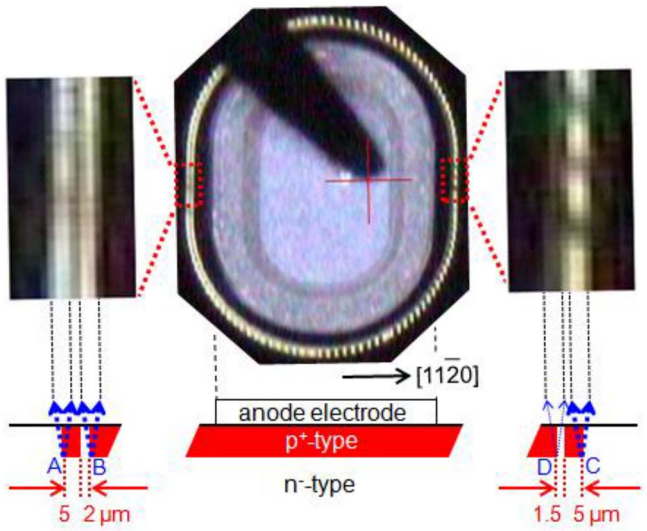

FIGURE 8. Photographically recorded light emission from the diode with *d* of 1.5 μm operated at a reverse current of 10 mA, and a schematic cross section of the diode. A, B, and C are possible points from which strong light is emitted.

Avalanche capability of the fabricated diodes is yet to be measured; however, this observation indicates that avalanche ruggedness of AS-FFR-terminated p-n diodes was possibly improved compared to that of conventional FFR-terminated p-n diodes.

V. CONCLUSION

An asymmetrically spaced floating-field ring (AS-FFR) was found to be effective against non-uniform avalanche multiplication at 4H-SiC planar junctions formed on misoriented (0001) substrates. Luminescence at breakdown was nearly uniform when the spacing between the edge of the anode and the inner edge of the AS-FFR was 2.0 μm in the [$\bar{1}\,\bar{1}$20] direction and 1.5 μm in the [11$\bar{2}$0] direction. This result should contribute to exploring the possibility of 4H-SiC power devices with higher avalanche ruggedness.

REFERENCES

[1] B. J. Baliga, *Silicon Carbide Power Devices*. Hackensack, NJ, USA: World Scientific, 2005.
[2] S. T. Allen, R. A. Sadler, J. W. Palmour, and C. H. Carter, Jr., "Silicon carbide MESFETs for high-power S-band applications," in *Proc. IEEE MTT-S Dig.*, Denver, CO, USA, Jun. 1997, pp. 57–60.
[3] Y. M. Sung, J. B. Casady, J. B. Dufrene, and A. K. Agarwal, "A review of SiC static induction transistor development for high-frequency power amplifiers," *Solid-State Electron.*, vol. 46, pp. 605–613, May 2002.
[4] B. J. Baliga, *Fundamentals of Power Semiconductor Devices*. New York, NY, USA: Springer, 2008, pp. 91–155.
[5] Y. C. Kao and E. D. Wolley, "High-voltage planar p-n junctions," *Proc. IEEE*, vol. 55, no. 8, pp. 1409–1414, Aug. 1967.
[6] A. Kinoshita *et al.*, "Influence of surface roughness on breakdown voltage of 4H-SiC SBD with FLR structure," *Mater. Sci. Forum*, vols. 615–617, pp. 643–646, Mar. 2009.
[7] K. Mochizuki, H. Okino, H. Matsushima, and Y. Toyota, "Observation and analysis of a non-uniform avalanche phenomenon in 4H-SiC 4°-off (0001) p-n diodes terminated with a floating-field ring," *Mater. Sci. Forum*, vols. 821–823, pp. 640–643, May 2015.
[8] N. Kuroda, K. Shibahara, W. S. Yoo, S. Nishino, and H. Matsunami, "Step-controlled VPE growth of SiC single crystals at low temperatures," in *Proc. 19th Conf. Solid State Devices Mater.*, Tokyo, Japan, 1987, pp. 227–230.
[9] K. Mochizuki, T. Someya, T. Takahama, H. Onose, and N. Yokoyama, "Detailed analysis and precise modeling of multiple-energy Al implantations through SiO_2 layers into 4H-SiC," *IEEE Trans. Electron Devices*, vol. 55, no. 8, pp. 1997–2003, Aug. 2008.
[10] K. Mochizuki and N. Yokoyama, "Two-dimensional analytical model for concentration profiles of aluminum implanted into 4H-SiC (0001)," *IEEE Trans. Electron Devices*, vol. 58, no. 2, pp. 455–459, Feb. 2011.
[11] G. Lulli, "Two-dimensional simulation of undermask penetration in 4H-SiC implanted with Al^+ ions," *IEEE Trans. Electron Devices*, vol. 58, no. 1, pp. 190–194, Jan. 2011.
[12] E. Morvan *et al.*, "Lateral spread of implanted ion distributions in 6H-SiC: Simulation," *Mat. Sci. Eng. B*, vols. 61–62, pp. 373–377, Jul. 1999.
[13] K. Mochizuki, N. Kameshiro, H. Onose, and N. Yokoyama, "Influence of lateral spreading of implanted aluminum ions and implantation-induced defects on forward current-voltage characteristics of 4H-SiC junction barrier Schottky diodes," *IEEE Trans. Electron Devices*, vol. 56, no. 5, pp. 992–997, May 2009.
[14] R. Rupp *et al.*, "Avalanche behavior and its temperature dependence of commercial SiC MPS diodes: Influence of design and voltage class," in *Proc. 26th Int. Conf. Power Semicond. Devices ICs*, Waikoloa, HI, USA, 2014, pp. 67–70.
[15] X. Cheng *et al.*, "A general design methodology for the optimal multiple-field-limiting-ring structure using device simulator," *IEEE Trans. Electron Devices*, vol. 50, no. 10, pp. 2273–2279, Oct. 2003.
[16] K. Mochizuki, H. Okino, H. Matsushima, and R. Yamada, "A commercial-simulator-based numerical-analysis methodology for 4H-SiC power devices formed on misoriented (0001) substrates," *IEEE J. Electron Devices Soc*, DOI: 10.1109/JEDS.2015.2418785.
[17] (May 7, 2015). *Device Simulation*. [Online]. Available: http://www.synopsys.com/tools/tcad/Pages/default.aspx
[18] (May 7, 2015). *Atlas*. [Online]. Available: http://www.silvaco.com/products/tcad.html
[19] T. Hatakeyama *et al.*, "Impact ionization coefficients of 4H silicon carbide," *Appl. Phys. Lett.*, vol. 85, no. 8, pp. 1380–1382, Aug. 2004.
[20] K. Wada *et al.*, "Blocking characteristics of 2.2 kV and 3.3 kV-class 4H-SiC MOSFETs with improved doping control for edge termination," *Mater. Sci. Forum*, vols. 778–780, pp. 915–918, 2014.
[21] H. Okino *et al.*, "Electrical characteristics of large chip-size 3.3 kV SiC-JBS diodes," *Mater. Sci. Forum*, vols. 740–742, pp. 881–886, 2013.
[22] N. Kameshiro *et al.*, "Electrical characteristics of large chip-size 3.3 kV SiC-JBS diodes," in *Proc. 59th JSAP Spring Meeting*, Tokyo, Japan, 2012, Art. ID 18p-A8-5.
[23] S. Ono, M. Arai, and C. Kimura, "Ultrabroadband emission spectrum from a reverse-biased 4H-SiC p-n junction diode," *Jpn. J. Appl. Phys.*, vol. 43, no. 10, pp. 7107–7108, 2004.
[24] A. O. Konstantinov, Q. Wahab, N. Nordell, and U. Lindefelt, "Ionization rates and critical fields in 4H silicon carbide," *Appl. Phys. Lett.*, vol. 71, no. 1, pp. 90–92, Jul. 1997.

KAZUHIRO MOCHIZUKI (M'98–SM'99) received the B.E., M.E., and Ph.D. degrees in electronic engineering from the University of Tokyo, Tokyo, Japan, in 1986, 1988, and 1995, respectively.

Since 1988, he has been with the Central Research Laboratory, Hitachi, Ltd., Tokyo. He has contributed to advances in epitaxial growth, device, and modeling technologies for compound semiconductors, including InAlGaAsP, ZnMgSSe, AlGaN, and SiC. From 1999 to 2000, he was a Visiting Researcher with the University of California, San Diego, where he worked on tunneling-collector heterojunction-bipolar transistors. He has served as a Part-Time Lecturer with the University of Electro-Communications, Tokyo (2003–present), and Hosei University, Tokyo (2010–present).

Dr. Mochizuki is a member of the Japan Society of Applied Physics.

NORIFUMI KAMESHIRO received the M.E. degree in electronics engineering from Nagoya University, Nagoya, Japan, in 2003.

In 2003, he joined the Central Research Laboratory, Hitachi, Ltd., Tokyo, Japan, where he has been engaged in the research and development of semiconductor processes and devices.

HIROYUKI MATSUSHIMA received the B.E. and M.E. degrees in physical engineering from Nagoya University, Nagoya, Japan, in 2009 and 2011, respectively.

Since 2011, he has been with the Central Research Laboratory, Hitachi, Ltd., Tokyo, Japan. His major research interests include characteristics and reliability of SiC power devices.

HIROYUKI OKINO received the B.S., M.S., and Ph.D. degrees in physics from the University of Tokyo, Tokyo, Japan, in 2002, 2004, and 2007, respectively.

Since 2007, he has been with the Central Research Laboratory, Hitachi, Ltd., Tokyo. His major interest is reliability of power devices.

Dr. Okino is a member of the Japan Society of Applied Physics.

RENICHI YAMADA (M'01–SM'11) received the B.S., M.S., and Ph.D. degrees in physics from the University of Tokyo, Tokyo, Japan, in 1987, 1989, and 1993, respectively.

He was a Researcher with the University of Tokyo, for two years. He then joined the Central Research Laboratory, Hitachi, Ltd., Tokyo, in 1995. He was a Visiting Industrial Fellow with the University of California, Berkeley, from 2001 to 2002. His major research interests include reliability physics of very large-scale integration and power devices.

Dr. Yamada is a member of the Japan Society of Applied Physics.